Indazolato Derivatives of Boron, Aluminum, and Gallium: Characterization and Solvent-Dependent Regioisomeric Structures through $\pi-\pi$ Interactions in the Solid State

Sara A. Cortes-Llamas, Julio M. Hernández-Pérez, Minhhuy Hô, and Miguel-Ángel Muñoz-Hernández*

Centro de Investigaciones Químicas, Universidad Autónoma del Estado de Morelos, Av. Universidad 1001, Colonia Chamilpa, Cuernavaca, Morelos 62209, Mexico

Received July 28, 2005

The complexes $[(\eta^1{:}\eta^1\text{-ind})(\mu\text{-M})R_2]_2$ (R = Me, M = Ga (**1**); R = Me, M = Al (**2**); R = Et, M = B (**3**)) were prepared by treatment of indazole with MR_3 in toluene. These have dimeric molecular structures, with the indazolato ligands coordinated in a $\eta^1{:}\eta^1$ fashion. In solution, complexes **1** and **2** show a mixture of syn and anti isomers in a 3:5 ratio, respectively; however, in the solid state the anti isomers can be selectively crystallized in toluene and the syn isomers in benzene. These complexes constitute the first examples of organoaluminum and organogallium complexes for which both isomers observed in solution can be selectively crystallized. In contrast with **1** and **2**, for boron complex **3** only the anti isomer was observed in solution and in the solid state. Results from theoretical calculations at the B3LYP/6-31G* level and NBO analyses were performed to gain insight into the nature of the metal−ligand bond and into the question of whether $\pi-\pi$ interactions in the crystal packing play an important role in the molecular structure of the isomer crystallized.

Introduction

Recently, there has been considerable interest in the chemistry of pyrazolato complexes of group 13 elements.[1] The majority of these compounds contain bulky alkyl or aryl substituents in the 3- and 5-positions of the pyrazolato ligand. The indazole ligand indH, a 3,4-substituted pyrazole, has been used in the synthesis of poly(indazolyl)borato ligands.[2] The benzo ring fused to the pyrazole moiety opens the possibility to obtain complexes with different regiochemistry. For example, two isomers of the hydrotris(indazol-1-yl)borato ligand can be synthesized, Tp^{3Bo} and Tp^{4Bo}, depending on the substituents on the indazolato ligand.[2a] These indazolyl moieties also make it possible to assemble large noncovalent framework structures via $\pi-\pi$ interactions. For example, the complexes $[M(Tp^{4Bo})_2]$ (M = Fe, Co, Ni, Zn)[3] show porous framework structures constructed through C−H···π interactions in which the cavities are filled by solvent molecules.[2b] It came to our attention that, to date, the only example of a structurally characterized neutral indazolyl complex with group 13 elements is the gallium complex $[(\eta^1{:}\eta^1\text{-ind})(\mu\text{-Ga})Me_2]_2$ (**1**).[4] Our recent findings on the chemistry of polypyrazolylaluminates[5] motivated us to explore the indazolyl complexes of B and Al and reexamine the Ga complex **1**. Herein, we describe the synthesis and characterization of the neutral indazolato complexes $[(\eta^1{:}\eta^1\text{-ind})(\mu\text{-M})R_2]_2$ (R = Me, M = Ga (**1**); R = Me, M = Al (**2**); R = Et, M = B (**3**)). Depending on which solvent is used for the crystallization of **1** and **2**, the anti or syn isomer is selectively obtained as a unique product in the solid state. To our knowledge, this is the first example where isomeric indazolato complexes have been selectively crystallized.

Results and Discussion

The reaction of indH with $AlMe_3$ in toluene at room temperature affords in good yield the compound $[(\eta^1{:}\eta^1\text{-ind})(\mu\text{-Al})Me_2]_2$ (**2**) after crystallization from toluene/hexane. However, two isomers are possible: $\mathbf{2}_{anti}$ with a C_{2h} symmetry (all the methyl groups equivalent) and $\mathbf{2}_{syn}$ with a C_{2v} symmetry (two sets of chemically inequivalent methyl groups), as shown in Scheme 1.

The ^{1}H NMR spectrum of **2** in benzene-d_6 shows two sets of signals at 7.86−6.84 ppm, which are assigned to the protons attached to the indazolyl moiety, and three high-field signals at −0.02, −0.12, and −0.27 ppm in the ratio 3:10:3 assigned to the methyl protons (Figure 1). The latter suggests the coexistence of both isomers in solution. Further evidence was obtained from

* To whom correspondence should be addressed. E-mail: mamund2@buzon.uaem.mx.

(1) (a) Rendle, D. F.; Storr, A.; Trotter, J. *Can. J. Chem.* **1975**, *53*, 2944−2954. (b) Chang, C.-C.; Her, T.-Y.; Hsieh, F.-Y.; Yang, C.-Y.; Chiang, M. Y.; Lee, G.-H.; Wang, Y.; Peng, S.-M. *J. Chin. Chem. Soc.* **1994**, *41*, 783−789. (c) Lewinski, J.; Zachara, J.; Kopec, T.; Madura, I.; Prowotorow, I. *Inorg. Chem. Commun.* **1999**, *2*, 131−134. (d) Lewinski, J.; Zachara, J.; Gos, P.; Grabska, E.; Kopec, T.; Madura, I.; Marciniak, W.; Prowotorow, I. *Chem. Eur. J.* **2000**, *6*, 3215−3227. (e) Zheng, W.; Hohmeister, H.; Mösch-Zanetti, N. C.; Roesky, H. W.; Noltemeyer, M.; Schmidt, H. G. *Inorg. Chem.* **2001**, *40*, 2363−2367. (f) Zheng, W.; Mösch-Zanetti, N. C.; Blunck, T.; Roesky, H. W.; Noltemeyer, M.; Schmidt, H. G. *Organometallics* **2001**, *20*, 3299−3303.

(2) (a) Rheingold, A. L.; Haggerty, B. S.; Yap, G. P. A.; Trofimenko, S. *Inorg. Chem.* **1997**, *36*, 5097−5103. (b) Janiak, C.; Temizdemir, S.; Dechert, S.; Deck, W.; Girgsdies, F.; Heinze, J.; Kolm, M. J.; Scharmann, T. G.; Zipffel, O. M. *Eur. J. Inorg. Chem.* **2000**, 1229−1241. (c) Janiak, C.; Temizdemir, S.; Dechert, S. *Inorg. Chem. Commun.* **2000**, *3*, 271−275. (d) Craven, E.; Mutlu, E.; Lundberg, D.; Temizdemir, S.; Dechert, S.; Brombacher, H.; Janiak, C. *Polyhedron* **2002**, *21*, 553−562.

(3) $[M(Tp^{4Bo})_2]$ = bis[hydrotris(indazol-1-yl)borato]metal(II).

(4) (a) Rendle, D. F.; Storr, A.; Trotter, J. *Can. J. Chem.* **1975**, *53*, 2930−2943. (b) Peterson, L. K.; Thé, K. I. *Can. J. Chem.* **1979**, *57*, 2520−2522.

(5) Cortés-Llamas, S. A.; Velázquez-Carmona, M. A.; Muñoz-Hernández, M. A. *Inorg. Chem. Commun.* **2005**, *8*, 155−158.

10.1021/om0506421 CCC: $33.50
Publication on Web 01/06/2006

Scheme 1

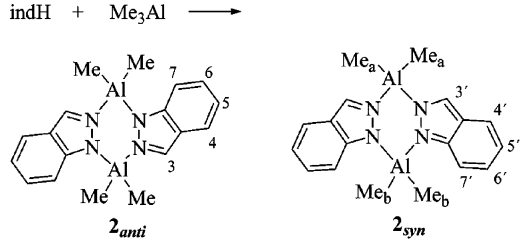

a ^{1}H-NOESY experiment of **2** (Figure 2). The methyl proton signal at −0.12 ppm suggests an intramolecular proximity with H-3 and with H-7, which we assigned to $\mathbf{2}_{anti}$. On the other hand, the signal at −0.02 ppm suggests an intramolecular proximity with H-3′ and the signal at −0.27 ppm with H-7′, in agreement with what is expected for Me_a and Me_b for $\mathbf{2}_{syn}$. Integration of these signals shows an approximate syn:anti ratio of 3:5, which is also observed in chloroform-*d*, THF-d_8, and toluene-d_8, in the temperature range of 353−193 K. Furthermore, the ^{13}C spectrum shows three signals at −6.74, −7.53, and −8.79 ppm assigned to the carbon atoms of the methyl groups and two sets of signals for the indazolyl moiety, which gives further confirmation of the presence of both isomers in solution. The signal of the ^{27}Al NMR appears to be too broad for observation.

Crystals suitable for X-ray diffraction studies were obtained for **2** from toluene at −20 °C. Remarkably, the isomer $\mathbf{2}_{anti}$ was crystallized as a unique product (Figure 3). We collected data for several different crystals from the same batch and also crystals from different batches of samples, but in all cases, only $\mathbf{2}_{anti}$ was observed. In addition, we collected data for the second crop of the crystallization in order to see if this was contaminated with the other isomer, but the anti isomer was again observed. Table 1 gives relevant data of the crystal collection, and Table 2 lists selected bond lengths and angles. The compound $\mathbf{2}_{anti}$ has a dimeric molecular structure, with the indazolato ligands coordinated in a η^1:η^1 fashion, forming a bridge between the two Al atoms. The total molecular structure consists of five fused rings, where the two benzo rings are oriented in opposite directions. The central six-membered ring N_4Al_2 has a planar conformation, and as a result, the five fused rings are coplanar. In $\mathbf{2}_{anti}$, the Al atoms are in a distorted-tetrahedral environment; the bond distances and angles (e.g., Al(1)−C(8) = 1.945(4) Å, Al(1)−N(2) = 1.932(4) Å, N(1)−Al(1)−N(2) = 102.48(18)°, and C(8A)−Al(1)−C(8) = 117.1(3)°) fall in the range of those observed in similar complexes; for example, in [(η^1:η^1-Me_2pz)-(μ-Al)Me_2]$_2$, Al(1)−C(1) = 1.947(3) Å, Al(1)−N(1) = 1.9244(17) Å, N(1)−Al(1)−N(2′) = 103.64(7)°, and C(1)−Al(1)−C(2) = 119.97(12)°.[1d] The existence of the isomers $\mathbf{2}_{anti}$ and $\mathbf{2}_{syn}$ in solution from the NMR data discussed above and the fact that the complex $\mathbf{2}_{anti}$ was selectively crystallized in toluene suggested to us that, under different conditions, the complex $\mathbf{2}_{syn}$ could be selectively crystallized. Thus, when crystals of **2** were grown from THF, $\mathbf{2}_{anti}$ was again obtained. However, when the crystallization of **2** was carried out in benzene, the isomer $\mathbf{2}_{syn}$ was obtained as the unique product. The molecular structure of $\mathbf{2}_{syn}$ is depicted in Figure 4. Selected bond distances and angles are presented in Table 2. The compound $\mathbf{2}_{syn}$ crystallizes in the orthorhombic crystal system, space group $Pna2_1$, with four molecules in the unit cell; one molecule of benzene was found in the crystal lattice for each molecule of $\mathbf{2}_{syn}$. As in $\mathbf{2}_{anti}$, the Al center is in a distorted-tetrahedral environment with Al(1)−C(16) = 1.962(2) Å, Al(1)−N(1) = 1.927(5) Å, N(1)−Al(1)−N(3) = 102.61(9)°, and C(15)−Al(1)−C(16) = 116.14(12)°. The six-membered ring Al_2N_4 shows an envelope conformation with an angle of 155.3° between the planes defined by the atoms N(1)−Al(1)−N(3) and N(2)−Al(2)−N(4).

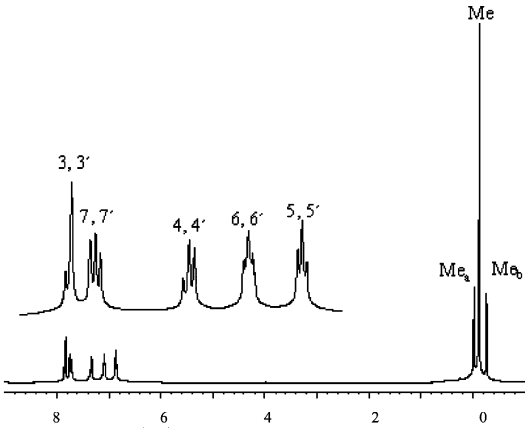

Figure 1. ^{1}H NMR spectrum of [(η^1:η^1-ind)(μ-Al)Me_2]$_2$ (**2**) at room temperature (benzene-d_6, 200 MHz), with the inset showing an expanded view of the chemical shift range from 8.0 to 6.8 ppm.

Crystals of $\mathbf{2}_{syn}$ dissolved in benzene-d_6, chloroform-*d*, or toluene-d_8 show the same ^{1}H NMR spectrum and the same pattern as discussed above, which indicates a mixture of the syn and anti isomers in a 3:5 ratio, respectively. The fact that the dissolution of crystals of $\mathbf{2}_{anti}$ and $\mathbf{2}_{syn}$ present the same NMR spectrum in solution suggests that an interconversion between the anti and syn isomers occurs. Dynamic exchanges have been observed in dinuclear organoaluminum compounds.[6] For example, in the complex [$Al(CH_3)_2(NHCH_2$-4-Py)]$_2$, the isomer with the two N−H groups trans to each other was crystallized from toluene.[6c] Nevertheless, both cis and trans isomers exist in solution in a 1:1 ratio. A similar situation was observed in the complexes [$R'_2AlN(H)SiR_3$]$_2$ (R′ = Me, ^{i}Bu; R = Ph, Et, ^{t}Bu), which undergo a cis−trans isomerization in solution with different cis:trans ratios depending on R′.[6b] However, to our knowledge **2** represents the first example of an organoaluminum complex in which both isomers can be selectively crystallized. We note that for **2** the solvent determines which isomer will crystallize; hence, the crystal packing could be responsible for this selectivity. The crystal structures of $\mathbf{2}_{anti}$ and $\mathbf{2}_{syn}$ show $\pi-\pi$ intermolecular interactions between the indazolato moieties and, moreover, for $\mathbf{2}_{syn}$ there are additional interactions with the benzene molecules included in the crystal lattice. Such $\pi-\pi$ interactions have been the subject of intensive studies due to their strong influence in the determination of the structure, stability, and crystal packing of the systems in which they participate.[7] Among the most common $\pi-\pi$ interactions are (i) *edge-to-face* or T-shaped interactions, which involves a perpendicular arrangement of aromatic rings, (ii) *offset stacked*, which is a parallel displaced arrangement, and (iii) the less common *face-to-face*, or sandwich, arrangement (Figure 5).[8]

In the crystalline structure of $\mathbf{2}_{anti}$, the molecules are organized in alternate layers with an ABABAB... arrangement. Between

(6) (a) Sierra, M. L.; Srini de Mel, J.; V.; Oliver, J. P. *Organometallics* **1989**, *8*, 2486−2488. (b) Choquette, D. M.; Timm, M. J.; Hobbs, J. L.; Rahim, M. M.; Ahmed, K. J.; Planalp, R. P. *Organometallics* **1992**, *11*, 529−534. (c) Trepanier, S. J.; Wang, S. *Organometallics* **1996**, *15*, 760−765.

(7) (a) Desiraju, G. R.; Gavezzotti, A. *J. Chem. Soc., Chem. Commun.* **1989**, 621−623. (b) Hunter, C. A.; Sanders, J. K. M. *J. Am. Chem. Soc.* **1990**, *112*, 5525−5534. (c) Müller-Dethlefs, K.; Hobza, P. *Chem. Rev.* **2000**, *100*, 143−167. (d) Hunter, C. A.; Lawson, K. R.; Perkins, J.; Urch, C. J. *J. Chem. Soc., Perkin Trans.* **2001**, *2*, 651−669.

(8) Meyer, E. A.; Castellano, R. K.; Diederich, F. *Angew. Chem., Int. Ed.* **2003**, *42*, 1210−1250.

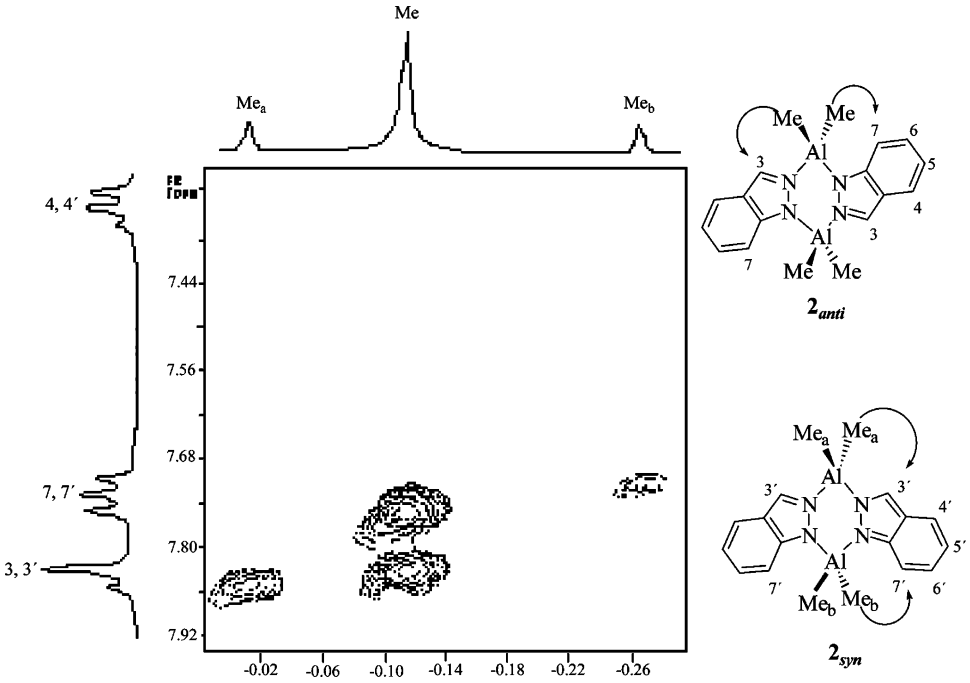

Figure 2. Section of the ^{1}H-NOESY spectrum of **2** recorded at 400 MHz in benzene-d_6, showing the intramolecular interactions between Al−Me and protons of the indazolato ligand.

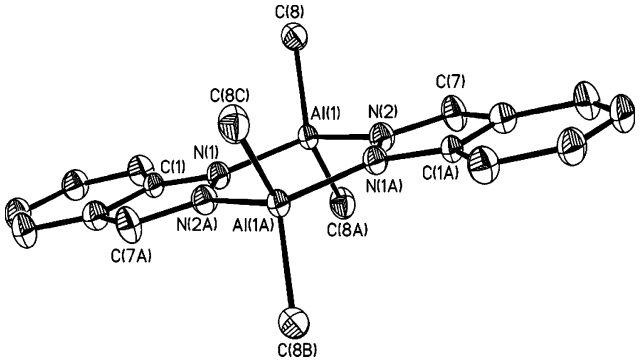

Figure 3. Perspective view of the complex $[(\eta^1{:}\eta^1\text{-ind})(\mu\text{-Al})Me_2]_2$ (**2**$_{anti}$), showing thermal ellipsoids at the 50% probability level (hydrogen atoms have been omitted for clarity).

these layers, the molecules show $\pi-\pi$ interactions with an *offset stacked* arrangement. Each molecule participates in four of these interactions, two with the molecules of the layer above and two with the layer below (d = 3.65 Å and R^1 = 1.32 Å) (Figure 6). The crystalline structure of **2**$_{syn}$ is made up of alternating parallel molecules stacked in an almost *face-to-face* geometry, forming double rows that run through axis c (d = 3.56 Å and R^1 = 0.68 Å). These double rows are separated in the a and b directions by benzene molecules, which are bonded to the indazolato complexes through *edge-to-face* interactions, with distances between 4.63 and 5.86 Å to the ring centroids, which are within the range reported[8] for these types of $\pi-\pi$ interactions (Figure 7).

In view of these results, we were interested in knowing whether such a control is kept in analogous complexes of group 13 elements. Since the interconversion between anti and syn isomers requires the breaking of the metal−nitrogen bond, we expected that it would be more difficult for complexes where the element−nitrogen bond is stronger (bond energy B−N = 93 kcal mol^{-1}, Al−N = 71 kcal mol^{-1}).[9] To ascertain this, we decided to prepare the gallium complex $[(\eta^1{:}\eta^1\text{-ind})(\mu\text{-Ga})Me_2]_2$ (**1**) and the boron ethyl complex $[(\eta^1{:}\eta^1\text{-ind})(\mu\text{-B})Et_2]_2$ (**3**). **1** has been previously synthesized from the reaction of $GaMe_3$ and 1 equiv of indH in refluxing benzene.[4a] Alternatively, we found that this reaction proceeds smoothly at room temperature in toluene. Remarkably, as in **2**, when **1** is crystallized, **1**$_{anti}$ is obtained from toluene and **1**$_{syn}$ from benzene. In both cases, the central ring Ga_2N_4 has a boat conformation (Figure 8). The crystallographic data obtained for compound **1**$_{anti}$ are identical with those reported by Storr et al.[4a] Table 1 gives relevant data of the crystal collection, and Table 2 lists selected bond lengths and angles. The compound **1**$_{syn}$ crystallizes in the orthorhombic crystal system, space group *Pbca*. The unit cell is made up by eight molecules of **1**$_{syn}$ and four molecules of benzene (Figure 8). The geometry about the gallium center may be described as distorted tetrahedral (Ga(1)−C(16) = 1.960(5) Å, Ga(1)−N(1) = 2.009(3) Å, N(1)−Ga(1)−N(3) = 97.18(13)°, and C(15)−Ga(1)−C(16) = 126.5(2)°). The crystal structure of **1**$_{anti}$ shows intermolecular interactions between pairs of molecules in an *offset stacked* arrangement (d = 3.50 Å, R^1 = 1.57 Å) (Figure 9), whereas in **1**$_{syn}$ the neighbors are nonparallel and show *edge-to-face* interactions between the gallium indazolato complexes and benzene. Each benzene molecule shows *edge-to-face* interactions with four indazolato moieties. The shortest ring-centroid to ring-centroid contacts are benzene−R5 = 4.89 Å (81.4°) and benzene−R6 = 5.12 Å (81.2°) (Figure 10).[10] Similar to the case for complex **2**, when crystals of **1**$_{anti}$ or **1**$_{syn}$ are dissolved in benzene-d_6, chloroform-d, or toluene-d_8, the ^{1}H NMR spectrum shows a mixture of **1**$_{anti}$ and **1**$_{syn}$ in a 5:3 ratio.[11]

Reaction between triethylborane and indH ligand in toluene yields the boron complex **3** (Scheme 2). In this case, although the crystallization was carried out in toluene or benzene, **3**$_{anti}$ was obtained as a unique product, as revealed by single-crystal X-ray crystallography. The molecular structure of **3**$_{anti}$ is given in Figure 11; relevant data of the crystal collection is presented

(9) Gaydon, A. G. *Dissociation Energies and Spectra of Diatomic Molecules*, 3rd ed.; Chapman and Hall: London, 1968.

(10) R5 corresponds to the five-membered pyrazole-type ring, and R6 corresponds to the six-membered annelated aryl ring of the indazolato group.

(11) It is worth mentioning that Peterson and Thé[4b] reported only the anti isomer for compound **1** in chloroform-d solution.

Table 1. Summary of Crystallographic Data for Complexes $\mathbf{1}_{anti}$, $\mathbf{1}_{syn}$, $\mathbf{2}_{anti}$, $\mathbf{2}_{syn}$, and $\mathbf{3}_{anti}$

	$\mathbf{1}_{anti}$	$\mathbf{1}_{syn}$	$\mathbf{2}_{anti}$	$\mathbf{2}_{syn}$	$\mathbf{3}_{anti}$
formula	$C_{18}H_{22}Ga_2N_4$	$C_{18}H_{22}Ga_2N_4$	$C_{18}H_{22}Al_2N_4$	$C_{18}H_{22}Al_2N_4$	$C_{22}H_{30}B_2N_4$
fw	433.88	433.88	348.36	348.36	372.18
cryst syst	orthorhombic	orthorhombic	monoclinic	orthorhombic	monoclinic
space group	*Pbca*	*Pbca*	*C*2/*m*	*Pna*2$_1$	*P*2$_1$/*n*
a (Å)	15.497(3)	8.9727(18)	15.820(4)	13.004(3)	17.243(4)
b (Å)	8.7580(14)	17.608(3)	7.2907(17)	10.787(2)	8.693(2)
c (Å)	27.081(5)	26.764(5)	8.5398(19)	16.481(4)	18.430(4)
α (deg)	90.0	90.0	90.0	90.0	90.0
β (deg)	90.0	90.0	111.805(4)	90.0	115.279(3)
γ (deg)	90.0	90.0	90.0	90.0	90.0
V (Å^3)	3675.4(11)	4228.4(14)	914.5(4)	2311.7(9)	2497.9(10)
Z	7	8	2	4	4
D_{calcd} (g/cm^3)	1.568	1.486	1.265	1.225	1.229
F(000)	1760	1928	368	904	992
cryst size (mm^3)	0.30 × 0.31 × 0.28	0.25 × 0.25 × 0.30	0.28 × 0.31 × 0.24	0.28 × 0.31 × 0.30	0.33 × 0.25 × 0.30
temp (K)	100	100	100	100	100
2*θ* range (deg)	2.78−25.00	2.31−27.02	2.57−24.98	2.26−26.97	2.23−28.31
no. of collected rflns	34 750	4457	2990	12 593	8457
no. of indep rflns	1829 (*R*(int) = 0.0957)	3538 (*R*(int) = 0.0223)	861 (*R*(int) = 0.0356)	4941 (*R*(int) = 0.0437)	4732 (*R*(int) = 0.0319)
no. of obsd rflns	1413 ($F > 4.0\ \sigma(F)$)	2779 ($F > 4.0\ \sigma(F)$)	786 ($F > 4.0\ \sigma(F)$)	3857 ($F > 4.0\ \sigma(F)$)	3551 ($F > 4.0\ \sigma(F)$)
no. of params	229	248	71	275	315
R	0.0609	0.0451	0.0704	0.0526	0.0493
R_w	0.1429	0.0982	0.1675	0.1154	0.1248
GOF	0.998	1.039	1.238	1.051	1.074
max, min diff electron density (e/Å^3)	1.132, −0.692	0.652, −0.422	0.553, −0.268	0.491, −0.219	0.274, −0.255

Table 2. Selected Bond Lengths (Å) and Angles (deg) for Complexes $\mathbf{1}_{anti}$, $\mathbf{1}_{syn}$, $\mathbf{2}_{anti}$, $\mathbf{2}_{syn}$, and $\mathbf{3}_{anti}$

Complex $\mathbf{1}_{anti}$

Ga(1)−N(2)	1.990(6)	N(1)−N(2)	1.391(9)
Ga(1)−N(4)	1.993(8)	N(3)−N(4)	1.373(8)
Ga(1)−C(15)	1.959(9)	N(3)−C(1)	1.356(11)
Ga(1)−C(16)	1.959(9)	N(4)−C(7)	1.347(9)
N(2)−Ga(1)−N(4)	99.1(3)	C(7)−N(4)−N(3)	107.8(7)
C(16)−Ga(1)−C(15)	124.3(4)	C(15)−Ga(1)−N(2)	108.8(3)
N(1)−N(2)−Ga(1)	123.7(7)	C(1)−N(3)−Ga(2)	127.1(5)
C(1)−N(3)−N(4)	107.9(5)		

Complex $\mathbf{1}_{syn}$

Ga(1)−N(1)	2.009(3)	N(2)−N(1)	1.379(5)
Ga(1)−N(3)	2.010(3)	N(3)−N(4)	1.370(5)
Ga(1)−C(15)	1.957(5)	N(1)−C(7)	1.327(6)
Ga(1)−C(16)	1.960(5)	N(2)−C(1)	1.376(5)
N(1)−Ga(1)−N(3)	97.18(13)	C(1)−N(2)−N(1)	106.5(4)
C(15)−Ga(1)−C(16)	126.5(2)	C(1)−N(2)−Ga(2)	127.7(3)
N(2)−N(1)−Ga(1)	125.2(3)	C(15)−Ga(1)−N(3)	109.93(17)
C(7)−N(1)−N(2)	110.1(3)		

Complex $\mathbf{2}_{anti}$

Al(1)−N(1)	1.904(4)	N(2)−C(7)	1.338(7)
Al(1)−N(2)	1.932(4)	N(2)−N(1)#2	1.366(6)
Al(1)−C(8)#1	1.945(4)	N(1)−N(2)#2	1.366(6)
Al(1)−C(8)	1.945(4)	N(1)−C(1)	1.368(6)
N(1)−Al(1)−N(2)	102.48(18)	N(1)#2−N(2)−Al(1)	129.7(3)
N(1)−Al(1)−C(8)#1	110.65(13)	N(2)#2−N(1)−C(1)	106.8(4)
C(8)#1−Al(1)−C(8)	117.1(3)	C(1)−N(1)−Al(1)	125.3(3)
C(7)−N(2)−N(1)#2	109.3(4)		

Complex $\mathbf{3}_{anti}$

B(1)−N(1)	1.575(2)	N(1)−N(2)	1.358(2)
B(1)−N(3)	1.600(2)	N(1)−C(1)	1.367(2)
B(1)−C(15)	1.611(2)	N(2)−C(7)	1.327(2)
B(1)−C(17)	1.602(3)		
C(17)−B(1)−C(15)	116.03(15)	C(15)−B(1)−N(3)	110.32(13)
C(17)−B(1)−N(1)	109.78(13)	N(1)−B(1)−N(3)	106.24(14)
C(17)−B(1)−N(3)	106.46(13)	B(1)−N(1)−N(2)	126.24(13)
C(15)−B(1)−N(1)	107.60(14)		

in Table 1, and Table 2 gives selected bond lengths and angles. The compound $\mathbf{3}_{anti}$ has a dimeric molecular structure and crystallizes in the monoclinic crystal system. The central six-membered ring N_4B_2 has a almost planar conformation, and the geometry of the boron center may be described as a distorted tetrahedron (B(1)−N(1) = 1.575(2) Å, B(1)−C(15) = 1.611(2) Å, N(1)−B(1)−N(3) = 106.24(14)°, and C(15)−B(1)−C(17) = 116.03(15)°). The multinuclear NMR data of crystals of $\mathbf{3}_{anti}$ dissolved in chloroform-*d* are consistent with the presence of only one isomer, namely $\mathbf{3}_{anti}$ (one set of signals for the aromatic protons and one set for the ethyl groups; Figure 12).

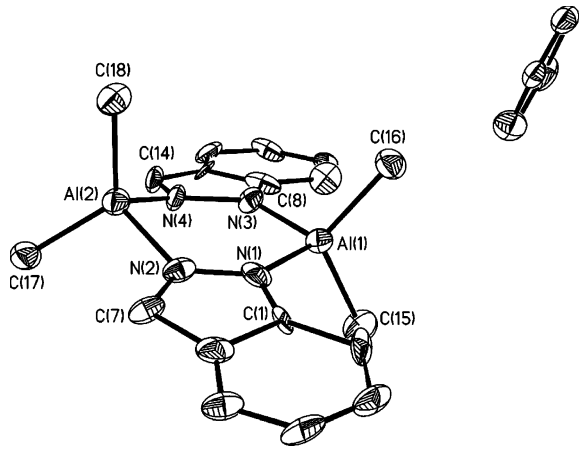

Figure 4. Perspective view of the complex $[(\eta^1{:}\eta^1\text{-ind})(\mu\text{-Al})Me_2]_2$ ($\mathbf{2}_{syn}$), showing thermal ellipsoids at the 50% probability level (hydrogen atoms have been omitted for clarity).

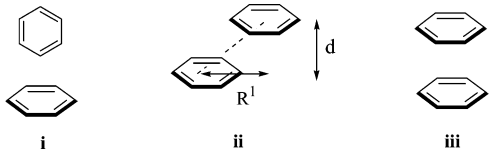

Figure 5. (i) *edge-to-face*, (ii) *offset stacked*, and (iii) *face-to-face* interactions. *d* is the distance between planes, and R^1 is the lateral offset.

The results observed for complexes **1**−**3** are summarized in Table 3. To have a better understanding of these results, ab initio calculations were performed at the B3LYP/6-31G* level, employing the Gaussian 98 suite of programs.[12] Geometric

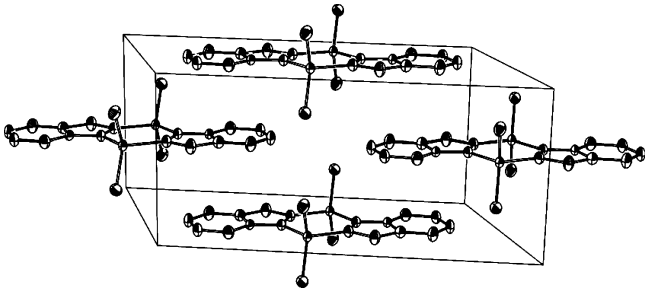

Figure 6. Perspective view of the unit cell of $[(\eta^1{:}\eta^1\text{-ind})(\mu\text{-Al})\text{-Me}_2]_2$ (**2**$_{anti}$), showing thermal ellipsoids at the 50% probability level (hydrogen atoms have been omitted for clarity).

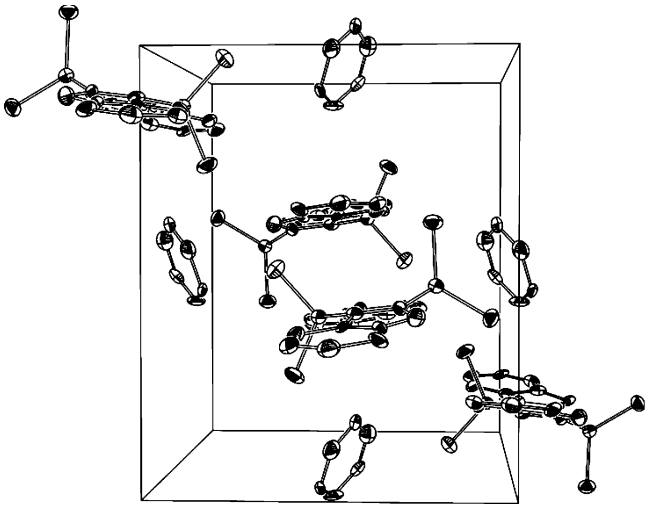

Figure 7. Perspective view of the unit cell of $[(\eta^1{:}\eta^1\text{-ind})(\mu\text{-Al})\text{-Me}_2]_2$ (**2**$_{syn}$), showing thermal ellipsoids at the 50% probability level (hydrogen atoms have been omitted for clarity).

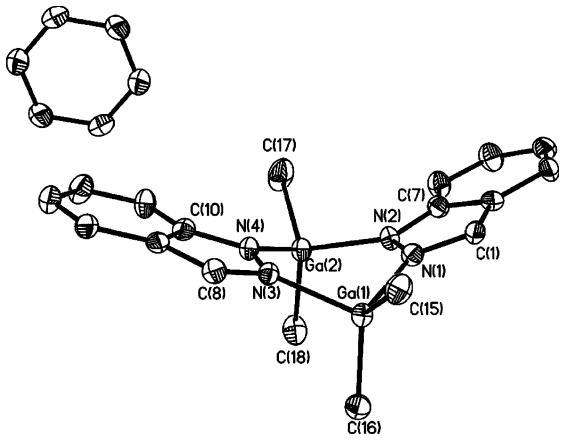

Figure 8. Perspective view of the complex $[(\eta^1{:}\eta^1\text{-ind})(\mu\text{-Ga})\text{-Me}_2]_2$ (**1**$_{syn}$) and a molecule of benzene, showing thermal ellipsoids at the 50% probability level (hydrogen atoms have been omitted for clarity).

parameters for **1**−**3** were obtained from single-crystal X-ray data. Molecular structures were fully optimized, and the stationary points were characterized as local minima by frequency calculations. For **1** and **2**, the anti isomer is more stable than the syn isomer; nevertheless, the difference is small (1.28 and 1.61 kcal/mol for **1** and **2**, respectively). These calculations seem to support the idea that both isomers for **1** and **2** coexist in solution, with the anti isomer in a slightly larger proportion than the syn isomer. On the other hand, for **3**, the calculation shows that the syn isomer is somewhat more stable

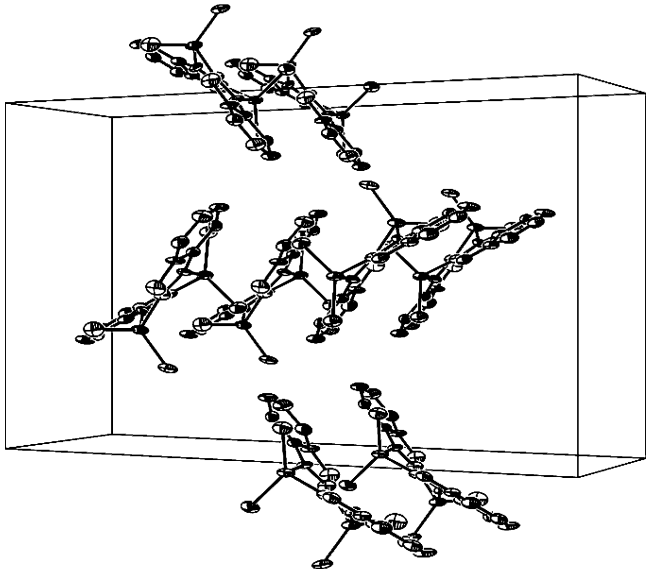

Figure 9. Perspective view of the unit cell of $[(\eta^1{:}\eta^1\text{-ind})(\mu\text{-Ga})\text{-Me}_2]_2$ (**1**$_{anti}$), showing thermal ellipsoids at the 50% probability level (hydrogen atoms have been omitted for clarity).

than the anti isomer (0.41 kcal/mol); however, only the anti isomer is observed experimentally. **1** and **2** were prepared at room temperature, while **3** was synthesized in refluxing toluene, due to the fact that BEt_3 and indH do not react at room temperature. This synthesis at toluene reflux temperature, as well as the stronger B−N bond energy (which makes it less likely for **3** to undergo an interconversion between anti and syn than for **1** and **2**),[9] may be the reason for the preferential isolation of the anti isomer. However, as shown in Table 3, each isomer can take different conformations: planar, envelope, and boat. It has been shown that in the related organoaluminum and gallium pyrazolato complexes $[(\eta^1{:}\eta^1\text{-R}_2\text{pz})(\mu\text{-M})\text{R}'_2]_2$ (M = Al, Ga) the conformation of the central ring depends on the nature of R and R′. For example, when R = H, R′ = Me[1b] the central ring has a boat shape, when R = Me, R′ = Me[1d] and R = H, R′ = ^{t}Bu,[1c] the heterocycle N_4Al_2 is planar, and when R = ^{t}Bu, R′ = Me,[1e] the ring is twisted. In addition, Storr et al,[13] showed that the N_4Ga_2 heterocycle tends to adopt a planar conformation in order to release the steric repulsions between substituents in the complex $[(\eta^1{:}\eta^1\text{-Me}_2\text{pz})(\mu\text{-Ga})\text{Me}_2]_2$. The fact that the central metallacycle here displays various conformations even though **1**−**3** have the same substituents indicates that other factors, as will be shown below, such as the nature of the metal−ligand bond and the $\pi-\pi$ interactions in the crystal packing play an important role.

For the anti isomers in **1** and **2**, the calculations show that the boat conformation has the lowest energy, whereas for **3** the planar conformation is more stable. We also optimized the geometry of the planar conformation for the anti isomer of **1**

(12) Frisch, M. J.; Trucks, G. W.; Schlegel, H. B.; Scuseria, G. E.; Robb, M. A.; Cheeseman, J. R.; Zakrzewski, V. G.; Montgomery, J. A., Jr.; Stratmann, R. E.; Burant, J. C.; Dapprich, S.; Millam, J. M.; Daniels, A. D.; Kudin, K. N.; Strain, M. C.; Farkas, O.; Tomasi, J.; Barone, V.; Cossi, M.; Cammi, R.; Mennucci, B.; Pomelli, C.; Adamo, C.; Clifford, S.; Ochterski, J.; Petersson, G. A.; Ayala, P. Y.; Cui, Q.; Morokuma, K.; Malick, D. K.; Rabuck, A. D.; Raghavachari, K.; Foresman, J. B.; Cioslowski, J.; Ortiz, J. V.; Stefanov, B. B.; Liu, G.; Liashenko, A.; Piskorz, P.; Komaromi, I.; Gomperts, R.; Martin, R. L.; Fox, D. J.; Keith, T.; Al-Laham, M. A.; Peng, C. Y.; Nanayakkara, A.; Gonzalez, C.; Challacombe, M.; Gill, P. M. W.; Johnson, B. G.; Chen, W.; Wong, M. W.; Andres, J. L.; Head-Gordon, M.; Replogle, E. S.; Pople, J. A. *Gaussian 98*, revision A.x; Gaussian, Inc.: Pittsburgh, PA, 1998.

(13) Rendle, D. F.; Storr, A.; Trotter, J. *Can. J. Chem.* **1975**, *53*, 2944.

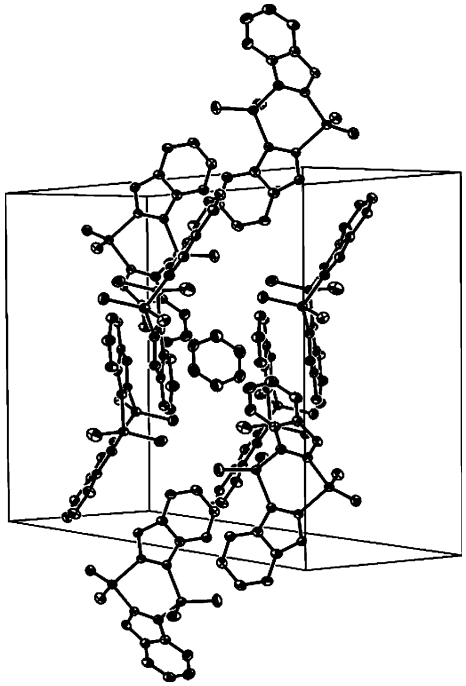

Figure 10. Perspective view of the unit cell of $[(\eta^1{:}\eta^1\text{-ind})(\mu\text{-Ga})\text{-}Me_2]_2$ (**1**$_{syn}$), showing thermal ellipsoids at the 50% probability level (hydrogen atoms have been omitted for clarity).

Scheme 2

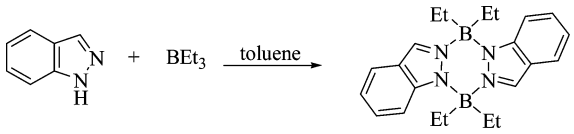

3$_{anti}$

and **2** and observed energy differences of 2.65 and 1.75 kcal/mol for **1** and **2**, respectively, with the boat conformation being more stable. These calculations show the same trend that is observed experimentally for **1** and **3** (**1** has the boat conformation and **3** is planar). For compound **2**, on the other hand, the experimental conformation observed is planar, which is not in agreement with the calculation. This result could be explained in terms of the small difference in calculated energies of the planar and boat conformations in isolated molecules. Thus, an evaluation of the packing effect was approximated by calculating the energy difference between a cluster of four monomers, whose geometry was taken directly from X-ray data, and that of four noninteracting monomers. The results show that, in contrast to the single-molecule calculation, each monomer gains 0.36 kcal/mol being planar in the cluster. We suggest that this extra stability comes from the $\pi-\pi$ interactions between the *offset stacked* aromatic rings, which are 3.65 Å apart. Previous studies of interactions of aromatic rings show a typical interplanar distance in the range 3.4−3.6 Å and an energy gain of 2.46 kcal/mol.[14] Here, compound **2** shows a smaller gain, which reflects the fact it has also to overcome an energy barrier of 1.75 kcal/mol to be planar.

We performed a natural bond orbital (NBO) analysis,[15] a process which localizes the molecular orbital in order to facilitate

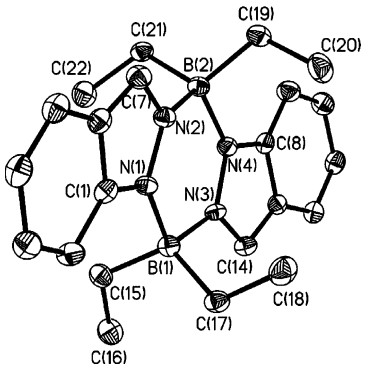

Figure 11. Perspective view of the complex $[(\eta^1{:}\eta^1\text{-ind})(\mu\text{-B})\text{-}Et_2]_2$ (**3**), showing thermal ellipsoids at the 50% probability level (hydrogen atoms have been omitted for clarity).

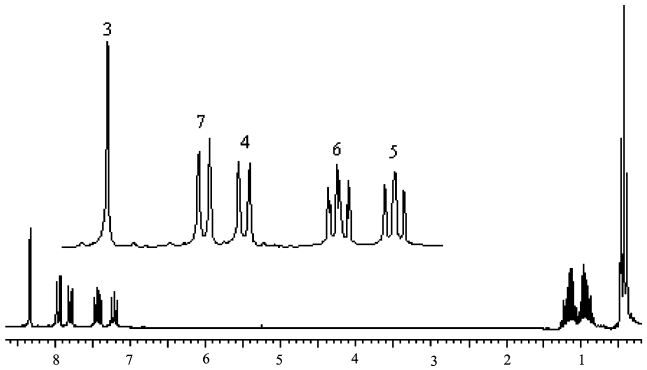

Figure 12. ^{1}H NMR spectrum of $[(\eta^1{:}\eta^1\text{-ind})(\mu\text{-B})Et_2]_2$ (**3**) at room temperature (chloroform-*d*, 200 MHz), with the inset showing an expanded view of the chemical shift range 8.6−7.1 ppm.

Table 3. Conformations of the Central Ring M_2N_4 from X-ray Data for 1−3 and Isomers in Solution

compd	isomers in soln	N_4M_2 (conformation)
$[(\eta^1{:}\eta^1\text{-ind})(\mu\text{-Ga})Me_2]_2$ (**1**)	syn/anti (3:5)	anti (boat) syn (boat)
$[(\eta^1{:}\eta^1\text{-ind})(\mu\text{-Al})Me_2]_2$ (**2**)	syn/anti (3:5)	anti (planar) syn (envelope)
$[(\eta^1{:}\eta^1\text{-ind})(\mu\text{-B})Et_2]_2$ (**3**)	anti	(planar)

interpretations of conventional chemical concepts such as hybridization, hyperconjugation, etc., to study the bonding scheme of the central ring M_2N_4 in complexes **1**−**3**. The results show that, in the cases of aluminum and gallium, the overlap between the unoccupied orbitals of these metals and the lone pair of electrons of the nitrogen atoms is enhanced by the boat conformation, whereas in the case of boron, such an interaction is not observed. Instead, NBO analysis shows that bonding orbitals of boron resemble a hybridization of the type sp^3 and the nitrogen atoms with a sp^2 hybridization, favoring a planar conformation. Indeed, in the X-ray crystal structure of **3**, the N−B−N angle has a average value of 106.07°; meanwhile in compound **1** the N−Ga−N average angle is 98.84°, closer to the value of an angle formed by nonhybridized p orbitals.

All complexes discussed so far crystallize in monoclinic or orthorhombic crystal systems, and the shortest crystallographic axes (8.758, 8.973, 7.291, 10.787, and 8.693 Å for **1**$_{anti}$, **1**$_{syn}$, **2**$_{anti}$, **2**$_{syn}$, and **3**, respectively) are parallel to a screw-axis symmetry operation. Interestingly, this was also observed in polyaromatic hydrocarbons and suggests the extension of the four packing systems proposed by Desiraju and Gavezzotti[7a] to complexes **1**−**3**. Consequently, **2**$_{anti}$ shows *offset stacking* interactions in a ABABAB... arrangement, forming "graphitic"

(14) Tsuzuki, S.; Honda, K.; Uchimaru, T.; Mikami, M.; Tanabe, K. *J. Am. Chem. Soc*. **2002**, *124*, 104.

(15) Glendening, E. D.; Badenhoop, J. K.; Reed, A. E.; Carpenter, J. E.; Bohmann, J. A.; Morales, C. M.; Weinhold, F. NBO 5.0; Theoretical Chemistry Institute, University of Wisconsin, Madison, WI, 2001.

planes characteristic of the *β packing*. There are $\pi-\pi$ interactions in $\mathbf{1}_{anti}$ between pairs of molecules, and these pairs are arranged in a *γ packing* system. In the structures of $\mathbf{1}_{syn}$ and $\mathbf{3}_{anti}$ the neighboring molecules are nonparallel and show only *edge-to-face* interactions consistent with a *herringbone packing* system. The structure of $\mathbf{2}_{syn}$ shows sandwich-like diads and also *edge-to-face* interactions consistent with the *sandwich-herringbone packing* system. It is worthwhile to point out that the shortest crystallographic axes in **1**−**3** are longer than in the Desiraju and Gavezzotti classification, due to the presence of alkyl groups bonded to the metal atoms that increase the size of the unit cell.

Summary and Conclusions

We have found that, in solution, the complexes **1** and **2** show a mixture of syn and anti isomers in the ratio 3:5, respectively. However, the anti isomers can be selectively crystallized in toluene and syn isomers in benzene. In agreement with these result, theoretical calculations showed that the anti isomer is more stable than the syn isomer but the energetic difference between the anti and syn isomers is small; therefore, the selectively crystallized isomer could be determined by the $\pi-\pi$ interactions present in the crystal structure. In contrast, for compound **3**, only the anti isomer is observed as a liquid as well as in the solid state, independent of the crystallization solvent. Most likely, this stems from two factors: for instance, the stronger B−N bond energy as compared those for Al and Ga makes it difficult for the interconversion process between the anti and syn isomers to occur, and although calculations predict that both isomers should be isolable, the low reactivity of BEt_3 and IndH at room temperature limits the practical investigation of the reaction. On the other hand, although complexes **1**−**3** have the same indazolato ligand, the central ring N_4M_2 shows different conformations (planar, envelope, and boat). The observed conformations can be explained by factors such as the $\pi-\pi$ interactions in the crystal packing and the nature of the metallic center. The crystal structure of complexes **1**−**3** can be organized according to the Desiraju and Gavezzotti classification; these similitudes demonstrate how this classification for polyaromatic compounds could be extended to include organometallic complexes, such as **1**−**3**.

Experimental Section

General Procedures. All experiments were carried out under Ar using standard Schlenk techniques in conjunction with an inert-atmosphere glovebox. Toluene, benzene, and hexane were distilled from Na/benzophenone and stored under N_2 prior to use. Indazole was prepared as described in the literature.[16] A 1.0 M solution of triethylborane in hexane was used. All other chemicals were purchased from Aldrich and used as received. ^{1}H, ^{11}B, ^{13}C, and ^{27}Al NMR spectra were obtained on a Varian Gemini 200 MHz spectrometer (200 MHz for ^{1}H, 50.30 MHz for ^{13}C, 52 MHz for ^{27}Al, and 64.16 MHz for ^{11}B) at ambient probe temperature (293 K). ^{1}H and ^{13}C NMR chemical shifts were determined by reference to the residual solvent peaks. ^{27}Al NMR chemical shifts are reported vs $[Al(H_2O)_6]^{3+}$ in D_2O. Elemental analyses were obtained on a Bruker analyzer. IR data were recorded as KBr pellets on a FT-IR Bruker spectrometer and are reported in cm^{-1}.

Single-Crystal X-ray Crystallography. X-ray data for $\mathbf{1}_{anti}$, $\mathbf{1}_{syn}$, $\mathbf{2}_{anti}$, $\mathbf{2}_{syn}$, and $\mathbf{3}_{anti}$ were collected using the program SMART[17] on a Bruker APEX CCD diffractometer with monochromatized Mo Kα radiation ($\lambda = 0.710\ 73$ Å). Cell refinement and data reduction were carried out with the use of the program SAINT; the program SADABS was employed to make incident beam, decay, and absorption corrections in the SAINT-Plus version 6.0 suite.[18] Then, the structures were solved by direct methods with the program SHELXS and refined by full-matrix least-squares thechniques with SHELXL in the SHELXTL version 6.1 suite.[19] Hydrogen atoms were generated in calculated positions and constrained with the use of a riding model. The final models involved anisotropic displacement parameters for all non-hydrogen atoms. Further details of the structure analyses are given in Table 1.

[(η^1:η^1-ind)(μ-Ga)Me_2]$_2$ (1). A solution of Me_3Ga (0.29 g, 2.54 mmol) in 15 mL of toluene was slowly added to a stirred solution of indH (0.3 g, 2.54 mmol) in toluene (15 mL). The reaction mixture was stirred for 4 h at ambient temperature. After that, the volatiles were removed under vacuum, leaving a colorless residue, which was washed with hexane. When the crystallization was carried out in toluene (−20 °C), crystals of $\mathbf{1}_{anti}$ were isolated by cannula filtration and dried under dynamic vacuum (0.28 g, 80%), whereas when the solvent of crystallization was benzene (4 °C), $\mathbf{1}_{syn}$ was obtained (0.28 g, 80%). Mp: 133−135 °C. ^{1}H NMR (benzene-d_6, 25 °C): δ 7.74−7.63 (m, H-3, H-3′, H-7, and H-7′), 7.48−741 (m, H-4 and H-4′), 7.17−7.08 (m, H-6 and H-6′), 6.97−6.90 (m, H-5 and H-5′), 0.33 (s, Ga−CH_{3a} syn), 0.24 (s, Ga−CH_3 anti), 0.11 (s, Ga-Me_b syn). ^{1}H NMR (chloroform-*d*, 25 °C): δ 8.25 (s, H-3), 8.22 (s, H-3′), 7.79−7.67 (m, H-7, H-7′, H-4, and H-4′), 7.42−7.34 (m, H-6 and H-6′), 7.17−7.09 (m, H-5 and H-5′), 0.12 (s, Ga−CH_{3a} syn), 0.10 (s, Ga−CH_3 anti), 0.03 (s, Ga−Me_b syn). ^{1}H NMR (toluene-d_8, 25 °C): δ 7.79−7.69 (m, H-3, H-3′, H-7, and H-7′), 7.51−47 (m, H-4 and H-4′), 7.19−7.14 (m, H-6 and H-6′), 6.979−6.95 (m, H-5 and H-5′), 0.33 (s, Ga−CH_{3a} syn), 0.25 (s, Ga−CH_3 anti), 0.13 (s, Ga−Me_b syn). ^{13}C NMR (benzene-d_6, 25 °C): δ 149.06−114.11 (*ind*), −3.19 (Ga−CH_{3a} syn), −4.16 (Ga−CH_3 anti), −5.47 (Ga−CH_{3b} syn). IR (KBr, cm^{-1}): 3066 (w), 2963 (w), 1620 (w), 1505 (w), 1456 (w), 1394 (w), 1317 (w), 1259 (w), 1208 (w), 1151 (w), 1097 (s), 1022 (m), 907 (w), 818 (m), 790 (m), 745 (s), 634 (w), 585 (m), 540 (w), 432 (w). Anal. Calcd for $C_{18}H_{22}N_4Ga_2$: C, 49.83; H, 5.11; N, 12.91. Found: C, 49.66; H, 5.17; N, 12.92.

[(η^1:η^1-ind)(μ-Al)Me_2]$_2$ (2). In a procedure similar to that for the synthesis of **1**, indH (0.23 g, 1.97 mmol) and $AlMe_3$ (0.15 g, 1.97 mmol) were reacted in toluene (30 mL). Yield: 0.28 g (80%). As for **1**, when **2** was crystallized in toluene, $\mathbf{2}_{anti}$ was isolated, and in benzene, $\mathbf{1}_{syn}$ was crystallized. Mp: 168−169 °C. ^{1}H NMR (benzene-d_6, 25 °C): δ 7.86 (s, H-3′), 7.83 (s, H-3), 7.75−7.71 (m, H-7 and H-7′), 7.36−7.31 (m, H-4 and H-4′), 7.11−7.06 (m, H-6 and H-6′), 6.88−6.84 (m, H-5 and H-5′), −0.02 (s, Al−CH_{3a} syn), −0.12 (s, Al−CH_3 anti), −0.27 (s, Al−Me_b syn). ^{1}H NMR (chloroform-*d*, 25 °C): δ 8.47 (s, H-3), 8.43 (s, H-3′), 7.92−7.82 (m, H-4, H-4′, H-7, and H-7′), 7.53−7.49 (m, H-6 and H-6′), 7.21−7.25 (m, H-5 and H-5′), −0.34 (s, Al−CH_{3a} syn), −0.36 (s, Al−CH_3 anti), −0.44 (s, Al−Me_b syn). ^{1}H NMR (toluene-d_8, 25 °C): δ 7.95−7.79 (m, H-3, H3′, H7, and H7′), 7.45−7.41 (m, H-4 and H-4′), 7.20−7.14 (m, H-6 and H-6′), 6.99−7.92 (m, H-5 and H-5′), −0.01 (s, Al−CH_{3a} syn), −0.10 (s, Al−CH_3 anti), −0.22 (s, Al−Me_b syn). ^{13}C NMR (benzene-d_6, 25 °C): δ 149.64−114.29 (*ind*), −6.74 (Al−CH_{3a} syn), −7.53 (Al−CH_3 anti), −8.79 (Al−CH_{3b} syn). ^{27}Al NMR (benzene-d_6, 25 °C): δ 140.10 ($w_{1/2} = 4539$ Hz). IR (KBr, cm^{-1}): 2922 (m), 2888 (m), 2364 (s), 1930 (w), 1779 (w), 1662 (w), 1625 (m), 1563 (w), 1508 (m), 1460 (w), 1428 (w), 1402 (w), 1382 (w), 1319 (w), 1259 (w), 1191 (m), 1152 (w), 1129 (w), 1103 (s), 1031 (m), 941 (w), 909 (w), 823 (w), 791 (m), 756 (w), 738 (w), 677 (s), 579 (w), 460 (w), 426 (w). Anal. Calcd for

(16) Baumgarten, H. E. *Organic Syntheses*; Wiley: New York, 1973; Collect. Vol. 5, p 650.

(17) Sheldrick, G. M. SMART; Bruker AXS, Inc., Madison, WI, 2000.

(18) Sheldrick, G. M. SAINT-Plus 6.0; Bruker AXS, Inc., Madison, WI, 2000.

(19) Sheldrick, G. M. SHELXTL 6.10; Bruker AXS, Inc., Madison, WI, 2000.

$C_{18}H_{22}N_4Al_2$: C, 62.06; H, 6.37; N, 16.08. Found: C, 57.54; H, 5.99; N, 15.79.

[(η^1:η^1-ind)(μ-B)Et_2]$_2$ (3). To a stirred solution of indH (0.20 g, 1.69 mmol) in toluene (15 mL) was slowly added B(Et_3) (1.7 mL, 1.69 mmol) with a syringe at room temperature. The solution was refluxed for 24 h. After that, the solvent was reduced to 5 mL and stored at −20 °C. The solution deposited colorless crystals of **3** over time, which were isolated by cannula filtration and dried under dynamic vacuum (0.27 g, 85%). In this case, even the crystallization was carried out in toluene or benzene, the anti isomer was obtained. Mp: 176−177 °C. ^{1}H NMR (benzene-d_6, 25° C): δ 7.93 (d, 2H, H-7, $^3J_{H-H}$ = 8.4 Hz), 7.92 (s, 2H, H-3), 7.40 (d, 2H, H-4, $^3J_{H-H}$ = 8.5 Hz), 7.11 (t, 2H, H-6, $^3J_{H-H}$ = 8.5 Hz), 6.92 (t, 2H, H-5, $^3J_{H-H}$ = 8.5 Hz), 1.34 (dq, B−CH_{2a}, $^2J_{H-H}$ = 15.0 Hz, $^3J_{H-H}$ = 7.6 Hz), 1.05 (dq, B−CH_{2b}, $^2J_{H-H}$ = 15.0 Hz, $^3J_{H-H}$ = 7.6 Hz), 0.62 (t, B−CH_2−CH_3, $^3J_{H-H}$ = 7.6 Hz). ^{1}H NMR (chloroform-*d*, 25 °C): δ 8.32 (s, 2H, H-3), 7.95 (d, 2H, H-7, $^3J_{H-H}$ = 8.5 Hz), 7.80 (d, 2H, H-4, $^3J_{H-H}$ = 8.5 Hz), 7.43 (t, 2H, H-6, $^3J_{H-H}$ = 8.5 Hz), 7.21 (t, 2H, H-5, $^3J_{H-H}$ = 8.5 Hz), 1.16 (dq, B−CH_{2a}, $^2J_{H-H}$ = 15.0 Hz, $^3J_{H-H}$ = 7.6 Hz), 0.94 (dq, B−CH_{2b}, $^2J_{H-H}$ = 15.0 Hz, $^3J_{H-H}$ = 7.6 Hz), 0.43 (t, B−CH_2CH_3). ^{13}C NMR (chloroform-*d*, 25 °C): δ 142.31−114.76 (*ind*), 18.20 (B−*C*H_2), 9.59 (B−CH_2*C*H_3). ^{11}B NMR (chloroform-*d*, 25 °C): δ 4.29 ($w_{1/2}$ = 195 Hz). IR (KBr, cm^{-1}): 2947 (m), 2902 (m), 2866 (m), 1624 (w), 1511 (w), 1460 (m), 1427 (m), 1373 (w), 1331 (m), 1268 (m), 1234 (w), 1162 (m), 1141 (m), 1055 (s), 921 (m), 849 (m), 817 (m), 736 (m), 642 (w), 514 (w), 431 (w). Anal. Calcd for $C_{22}H_{30}N_4B_2$: C, 71.01; H, 8.13; N, 15.81. Found: C, 71.05; H, 8.12; N, 15.79.

Acknowledgment. We are indebted to the CONACYT-México (Grant J30234-E) for generous support of this work and Ph.D. grants to S.A.C.-L. and J.M.H.-P. Special thanks to Prof. J. García (FQ-UNAM) for helpful discussions and X-ray technical assistance.

Supporting Information Available: Crystallographic data are available as CIF files. This material is available free of charge via the Internet at http://pubs.acs.org.

OM0506421